Using SHRIMP zircon dating to unravel tectonothermal events in arc environments. The early Palaeozoic arc of NW Iberia revisited

Jacobo Abati,[1] Pedro Castiñeiras,[2] Ricardo Arenas,[1] Javier Fernández-Suárez,[1] Juan Gómez Barreiro[3] and Joseph L. Wooden[4]

[1]*Departamento de Petrología y Geoquímica, Universidad Complutense, 28040 Madrid, Spain;* [2]*Department of Geological Sciences, University of Colorado, Boulder, CO 80309, USA;* [3]*Department of Earth and Planetary Science, University of California, Berkeley, CA 94720-4767, USA;* [4]*USGS at Menlo Park, 345 Middlefield Road, Menlo Park, CA 94025, USA*

ABSTRACT

Dating of zircon cores and rims from granulites developed in a shear zone provides insights into the complex relationship between magmatism and metamorphism in the deep roots of arc environments. The granulites belong to the uppermost allochthonous terrane of the NW Iberian Massif, which forms part of a Cambro-Ordovician magmatic arc developed in the peri-Gondwanan realm. The obtained zircon ages confirm that voluminous calc-alkaline magmatism peaked around 500 Ma and was shortly followed by granulite facies metamorphism accompanied by deformation at c. 480 Ma, giving a time framework for crustal heating, regional metamorphism, deformation and partial melting, the main processes that control the tectonothermal evolution of arc systems. Traces of this arc can be discontinuously followed in different massifs throughout the European Variscan Belt, and we propose that the uppermost allochthonous units of the NW Iberian Massif, together with the related terranes in Europe, constitute an independent and coherent terrane that drifted away from northern Gondwana prior to the Variscan collisional orogenesis.

Introduction

The tectonothermal evolution of magmatic arcs is a key issue to understand the evolution of continental crust through time, as they are arguably the main geological setting for its formation and growth (e.g. Yoshino and Takamoto, 2004; Holbrook *et al.*, 1999). Many recent studies show that high-temperature metamorphism and magmatism in this enviromnent are closely related in space and time, showing a complex interplay where several thermal and/or deformational events can be developed in short time spans and show feedback relationships (Corona-Chávez *et al.*, 2006; Flowers *et al.*, 2005; McNulty, 1995). Thus, the relative chronology of the different processes involved is one of the main aspects that we need to investigate to constraint this evolution.

In this paper, we present the results of a U–Pb SHRIMP study of zircon from arc-related mafic and pelitic granulites. It is well known that zircon commonly retains age information of different geological events, which can be recorded in distinct domains of the crystal, typically cores and overgrowth rims. The meaningfulness of U–Pb ages obtained in the different domains depends on the correct interpretation of zircon internal features as revealed by cathodoluminescence (CL) or back-scattered electron images. When the age of the different zircon internal domains is relatively close, as could be expected in the high-grade rocks of arc systems, most U–Pb geochronological techniques cannot resolve their relative timing because they do not have the necessary precision. However, in this study we show that after a meticulous selection of samples and study of zircon internal features it is possible to date two high-grade events with an age difference of only *c.* 20 Ma, which approximates the resolution limit of the method.

The samples studied are two types of granulites belonging to the uppermost allochthon of the NW Iberian Massif, the most outboard terrane of the European Variscan Belt, considered part of a Cambro-Ordovician magmatic arc of peri-Gondwanan affinity (Abati *et al.*, 1999; Martinez Catalán *et al.*, 2002; Fernández-Suárez *et al.*, 2003). The first type of granulite is a metapelitic enclave in a large gabbro body, and the second type occurs as discrete shear zones in the basal part of the same gabbro. The crystallization age of the gabbro has already been established at 499 ± 2 Ma using U–Pb ID-TIMS (Abati *et al.*, 1999). The implications of these results for the general evolution of the European Variscan Belt will also be discussed.

Geological setting

The allochthonous terranes of the European Variscan Chain occur around suture zones that form a discontinuous belt running from the Iberian Massif to the Bohemian Massif in Eastern Europe. In NW Iberia, five allochthonous complexes (AC) are preserved in synforms between granitic and migmatitic gneiss domes (Fig. 1). Their geological features, geodynamic evolution and significance are described in detail elsewhere (e.g. Martínez Catalán *et al.*, 2002). These terranes are thrust upon autochthonous and parautochthonous sequences with northern Gondwanan affinities. From bottom to top, three units with distinct tectonometamorphic evolution can be correlated throughout the five AC: (1) Basal, (2) Ophiolitic and (3) Upper units.

Correspondence: Pedro Castiñeiras García, Profesor Ayudante, Departamento de Petrología y Geoquímica, Fac. CC, Geológicas, c/ José Antonio Nováis 2, 28040 Madrid, Spain. Tel.: +34 91 394 4898; fax: +34 91 544 2535; e-mail: castigar@geo.ucm.es

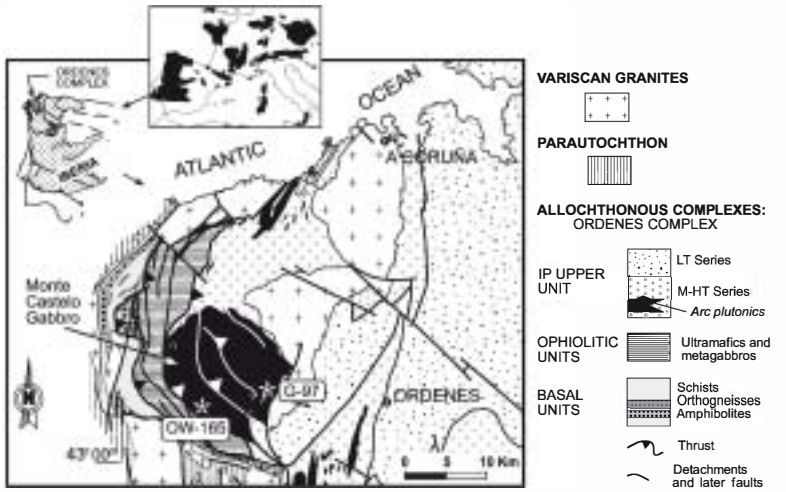

Fig. 1 Geological map of the NW Ordenes Complex showing the Monte Castelo gabbro and the location of the samples.

1 The Basal units consist of schists, paragneisses and early Ordovician felsic and mafic igneous rocks that underwent subduction and high-pressure (HP) metamorphism at 380–365 Ma during the closure of an oceanic realm (Martínez Catalán *et al*., 1996). They are considered to represent the external edge of the northern Gondwanan margin involved in the variscan collision.
2 Ophiolitic units highlight a rootless suture that marks the closure of the Palaeozoic Rheic Ocean (Martínez Catalán *et al*., 2002).
3 Overlying the ophiolites, the Upper units represent the most exotic terrane and form a complex pile that can be subdivided into a high-pressure and high-temperature sub-unit (HP–HT) in the lower part and an intermediate pressure (IP) sub-unit in the upper part. These units are viewed as parts of a magmatic arc, whose origin and evolution in the north Gondwana margin is closely linked with the opening of the Rheic Ocean (Andonaegui *et al*., 2002; Santos *et al*., 2002; Abati *et al*., 1999, 2003; Castiñeiras, 2005). This opening involved the previous development of an active margin and arc formation, as is suggested by the widespread arc development at that time in the Iapetus Ocean (van Staal *et al*., 1998; Winchester *et al*., 2002; van Staal, 2005). Probably, back-arc extension triggered the first stages of rifting, pulling apart the arc by slab roll back, and drifted away leaving behind a back-arc whose continued opening gave rise to the Rheic Ocean (Stampfli and Borel, 2002). The remnants of the arc are now preserved in the terranes outcropping above the ophiolites (the Upper units above the Rheic suture), and evidences of the back-arc extension and subsequent rifting are widespread in the terranes below them, like voluminous peralkaline magmatism (e.g. Pin *et al*., 1992).

This work focuses on the IP units (Fig. 1), because we consider that the original characteristics of the arc are best preserved in these units. The Upper units are interpreted as a section from the lower to upper part of a magmatic arc crust, thinned by extensional detachments and characterized by a complex polymetamorphic history. The HT–HP units are separated from the IP units by an important extensional detachment located on an earlier thrust plane (Díaz García *et al*., 1999). The lower part of the arc crust consists of a very heterogeneous sequence of ultramafic rocks, mainly harzburgites and pyroxenites (Girardeau and Gil Ibarguchi, 1991), eclogites, HP mafic granulites and HP paragneisses. The HP metamorphism was related to subduction during the accretion of the arc to the Laurentian margin in late Silurian–early Devonian times (425–390 Ma; Fernández-Suárez *et al*., 2002, 2007; Gómez Barreiro *et al*., 2006), although evidence for an earlier Cambrian to early Ordovician HT event is widespread (e.g. Fernández-Suárez *et al*., 2002). By contrast, in the overlying IP units, the regional metamorphism and tectonic fabrics are genetically related to the activity of the arc, therefore being older than the HP metamorphism. In summary, we have a lower section of the arc that was subducted in the late Silurian–early Devonian and was subsequently delaminated from its upper part, which still preserves most of the original magmatic, tectonic and metamorphic features of the arc, without a severe overprint of Variscan deformation or metamorphism.

The IP units consist of a thick metasedimentary pile (more than 9000 m) with metagreywackes, metapelites and conglomerates forming flyschoid sequences, intruded by numerous gabbroic and granodioritic bodies of different size. Excellent examples are the large Monte Castelo gabbro (Fig. 1) and the Corredoiras orthogneiss (Díaz García *et al*., 1999). Metamorphic grade decreases in intensity upwards, grading from IP granulite facies in the lower part of the unit to greenschist facies at the top. The largest plutons are generally undeformed and preserve igneous textures and mineralogy, the metamorphic mineral associations being restricted to the high-grade shear zones.

The metamorphic evolution of the lower granulitic part was studied in detail by Abati *et al*. (2003), and is characterized by an anticlockwise *P–T* path. After a high-*T*–low-*P* event caused by regional elevation of isotherms due to voluminous magmatism, the *P–T* path records an abrupt burial at high-*T* and subsequent cooling, yielding an anticlockwise loop. Similar paths are obtained at shallower crustal levels, in the medium-T metapelitic schists overlying the granulites (O Pino Schists; Castiñeiras, 2005). This kind of metamorphic evolution is well documented in magmatic arcs (e.g. Baba, 1998; Will and Schmädicke, 2003).

U–Pb results

We sampled two foliated granulites within the Monte Castelo gabbro. Sample G97 is a metapelitic

granulite-facies xenolith in the Monte Castelo gabbro. It consists of Grt + Opx + Bt + Pl + Qtz + Kfs + Crd + Sil + Rt ± Spn (mineral abbreviations after Kretz, 1983) and shows a complex texture with different micro-domains. In spite of the variety of zircon morphologies found in this sample, as expected for meta-sedimentary rocks, it is possible to distinguish two main sets. The first group is composed of variably worn out prisms with aspect ratios from 1 : 2 to 1 : 3 that we interpret as detrital grains. The second group consists of multifaceted grains, usually equant, that we interpret as new-grown metamorphic grains because this morphology is typical of zircons from granulite facies rocks (Corfu *et al.*, 2003; Harley *et al.*, 2007). CL images in the detrital grains (Fig. 2) reveal that most of the zircons have magmatic oscillatory zones, although some xenocrystic cores or thin dark rims (25–30 μm) can also be found. The multifaceted metamorphic zircons display a dark, faint, polygonal or sector zoning. Finally, some metamorphic zircons exhibit core-rim features, with sector zoning in both domains. A representative set of analytical data is listed in Table 1 (the complete set of data is provided as Electronic Appendices). Seventy-eight spots from 67 grains were analysed using the SHRIMP-RG at Stanford University (the analytical methods are described in an Electronic Appendix). The results reveal a few ages older than 700 Ma (Table 1), indicating that the original sedimentary rock has a probable Pan-African/Cadomian provenance (Figs 3a and 4a). Considering only the youngest ages, the relative probability curve has a peak at *c.* 500 Ma (Fig. 3b). Fifteen of the analyses that define this peak are obtained from metamorphic zircons and yield a mean age of 505.2 ± 2.4 Ma (mean square weighted deviation, MSWD 1.6, Fig. 4b).

Sample OW165 is a mafic granulite located in a shear zone cross-cutting the gabbro. It has granonematoblastic texture and a peak mineral assemblage formed by Grt + Opx + Pl + Hbl + Rt + Qtz. Zircon grains from this sample can be grouped in two sets. On the one hand, there are big prismatic grains (up to 0.5 mm), similar to those found in the gabbro (Abati *et al.*, 1999), which exhibit a variety of textures under CL, all of them characteristic of igneous rocks: homogeneous, fir-tree and sector zoning. On the other hand, there are small rounded grains, not found in the gabbro, which exhibit core-rim

Table 1 U Th Pb SHRIMP representative analytical data for zircons from the Monte Castelo granulitic shear zone (sample OW165) and the metapelitic granulite included in the Monte Castelo gabbro (sample G97).

Spot number		Common ^{206}Pb (%)	U (p.p.m.)	Th (p.p.m.)	$^{232}Th/^{238}U$	$^{238}U/^{206}Pb$*	$^{207}Pb/^{206}Pb$*	$^{238}U/^{206}Pb$†	$^{207}Pb/^{206}Pb$†	$^{206}Pb/^{238}U$‡	$^{206}Pb/^{238}U$§ age
Sample OW165											
2	DGC	<0.01	17	37	2.17	12.9512 ± 2.60	0.0537 ± 7.04	12.9344 ± 2.60	0.0548 ± 7.21	0.0775 ± 0.0021	481 ± 12
6.1	DGC	3.68	20	40	2.11	12.2580 ± 2.06	0.0868 ± 4.59	12.5139 ± 2.25	0.0705 ± 12.16	0.0786 ± 0.0017	488 ± 10
6.2	BR	<0.01	204	145	0.73	12.3151 ± 0.77	0.0570 ± 2.05	12.3350 ± 0.78	0.0557 ± 2.46	0.0812 ± 0.0006	503 ± 4
7.1	DGC	<0.01	15	16	1.15	11.9887 ± 2.31	0.0487 ± 7.13	11.6787 ± 2.72	0.0700 ± 17.47	0.0843 ± 0.0020	522 ± 12
7.2	BR	0.20	160	113	0.73	13.0117 ± 1.12	0.0582 ± 2.07	13.0117 ± 1.12	0.0582 ± 2.07	0.0767 ± 0.0009	476 ± 5
8.1	LGC	1.24	7	7	1.01	12.3400 ± 3.68	0.0672 ± 9.30	12.6025 ± 3.94	0.0501 ± 26.48	0.0800 ± 0.0031	496 ± 18
8.2	BR	0.05	283	168	0.61	12.9442 ± 0.59	0.0571 ± 1.67	12.9442 ± 0.59	0.0571 ± 1.67	0.0772 ± 0.0005	479 ± 3
9.1	LGC	0.92	10	8	0.90	12.4356 ± 3.17	0.0645 ± 8.32	13.2478 ± 3.82		0.0797 ± 0.0026	494 ± 16
9.2	BR	0.19	178	121	0.70	12.6429 ± 0.75	0.0585 ± 2.06	12.6645 ± 0.75	0.0571 ± 2.40	0.0789 ± 0.0006	490 ± 4
10.1	LGC	<0.01	6	4	0.66	12.4353 ± 3.65	0.0544 ± 10.38	13.2398 ± 4.36		0.0807 ± 0.0030	500 ± 18
10.2	BR	0.02	300	116	0.40	13.2026 ± 0.51	0.0566 ± 1.48	13.1998 ± 0.51	0.0568 ± 1.50	0.0757 ± 0.0004	471 ± 2
14	BR	0.32	266	166	0.64	12.8513 ± 0.58	0.0593 ± 1.56	12.8752 ± 0.59	0.0578 ± 2.01	0.0776 ± 0.0005	482 ± 3
Sample G97											
4.1	C	<0.01	754	695	0.95	10.4262 ± 0.44	0.0586 ± 1.09	10.4287 ± 0.44	0.0584 ± 1.11	0.0960 ± 0.0004	591 ± 3
4.2	R	0.03	164	42	0.27	12.2018 ± 1.13	0.0576 ± 3.14	12.2833 ± 1.13	0.0522 ± 4.10	0.0819 ± 0.0010	508 ± 6
5	DZ	<0.01	210	61	0.30	12.1658 ± 0.74	0.0563 ± 2.00	12.1658 ± 0.74	0.0563 ± 2.00	0.0823 ± 0.0006	510 ± 4
11	DZ	0.00	194	76	0.41	12.4629 ± 0.74	0.0572 ± 1.99	12.4629 ± 0.74	0.0572 ± 1.99	0.0802 ± 0.0006	498 ± 4
12	DZ	0.02	187	54	0.30	12.3486 ± 0.77	0.0574 ± 2.07	12.3795 ± 0.78	0.0554 ± 2.80	0.0810 ± 0.0006	502 ± 4
16	C	0.18	450	301	0.69	9.5137 ± 0.55	0.0626 ± 1.30	9.5237 ± 0.55	0.0617 ± 1.40	0.1049 ± 0.0006	643 ± 3
20	GZ	0.11	139	35	0.26	12.4534 ± 1.00	0.0580 ± 2.72	12.4953 ± 1.02	0.0553 ± 4.14	0.0802 ± 0.0008	497 ± 5
23	GC	0.40	137	43	0.32	12.2622 ± 1.17	0.0606 ± 4.06	12.3216 ± 1.29	0.0566 ± 9.02	0.0812 ± 0.0010	503 ± 6
27	DZ	0.03	1404	10	0.01	12.2479 ± 0.32	0.0576 ± 0.86	12.2467 ± 0.32	0.0577 ± 0.86	0.0816 ± 0.0003	506 ± 2
29	GZ	<0.01	137	36	0.27	12.5659 ± 1.17	0.0567 ± 3.22	12.6623 ± 1.27	0.0505 ± 8.63	0.0796 ± 0.0010	494 ± 6
36	DZ	<0.01	427	305	0.74	9.9321 ± 0.48	0.0594 ± 1.26	9.9619 ± 0.49	0.0569 ± 2.01	0.1008 ± 0.0005	619 ± 3
43.2	R	0.03	170	71	0.43	9.8329 ± 1.30	0.0608 ± 3.92	9.8865 ± 1.31	0.0563 ± 5.32	0.1017 ± 0.0014	624 ± 8
50.2	R	0.01	2015	404	0.21	9.6729 ± 0.29	0.0609 ± 0.68	9.6814 ± 0.29	0.0602 ± 0.80	0.1034 ± 0.0003	634 ± 2
66.2	R	<0.01	290	26	0.09	9.7161 ± 0.79	0.0590 ± 2.25	9.7979 ± 0.85	0.0521 ± 5.74	0.1031 ± 0.0008	633 ± 5

LGC, light grey core; DGC, dark grey core; BR, black rim; C, core; R, rim; GZ, grey zone; DZ, dark zone. All errors are 1σ.

*Uncorrected ratios.

†Radiogenic lead corrected for common lead using ^{204}Pb.

‡Radiogenic lead corrected for common lead using ^{207}Pb.

§Age obtained using the ^{207}Pb-corrected ratio.

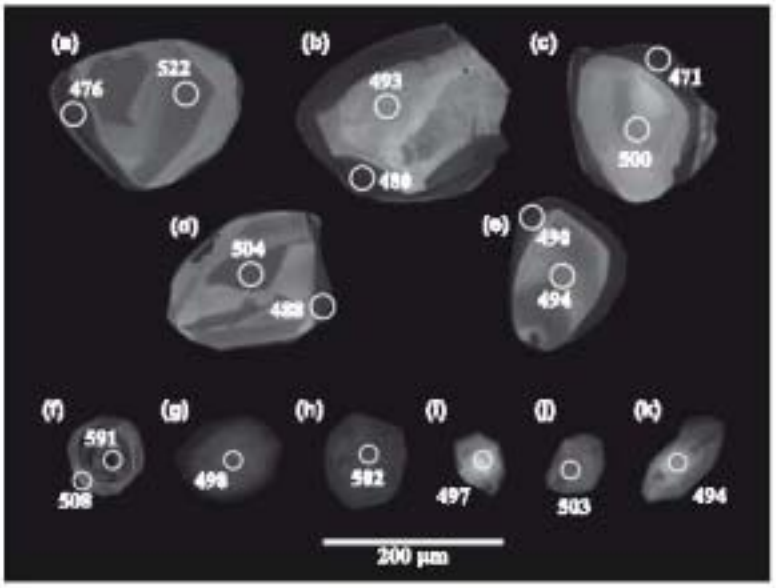

Fig. 2 Cathodoluminescence images of some of the analysed zircons with the location of the SHRIMP spots and the age in Ma; (a–e) zircon grains from sample GW165; (f–k) zircon grains from sample G97.

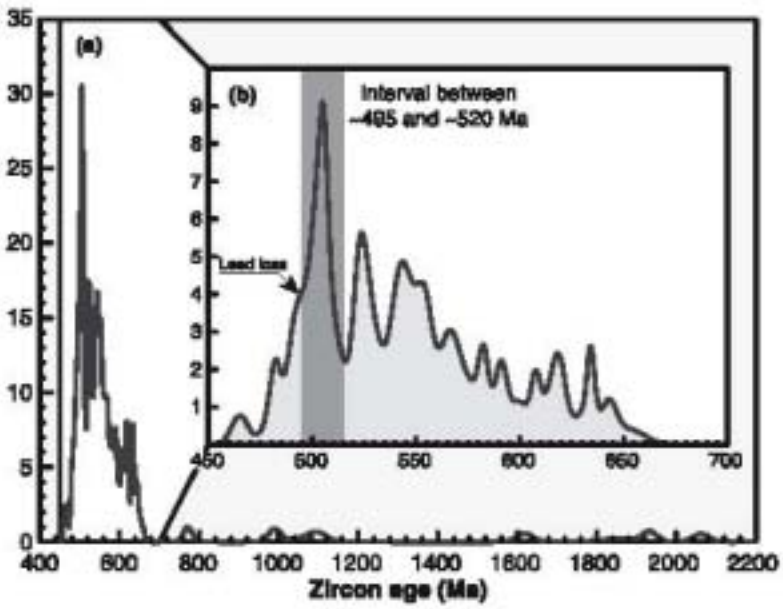

Fig. 3 (a) Relative probability plot for sample G97 showing all data, where ^{207}Pb-corrected $^{206}Pb/^{238}U$ ages were used for analyses younger than 1000 Ma, and ^{204}Pb-corrected $^{207}Pb/^{206}Pb$ for grains older than that value. (b) Relative probability plot for zircons younger than 700 Ma from sample G97. Young data were considered if common lead was less than 1%, whereas old data were included only if they were <10% discordant.

features, where a grey luminescent low U central zone with magmatic zoning is usually corroded and surrounded by non-luminescent overgrowths (Fig. 2). Twenty spots were analysed in 14 zircon grains (Table 1). Core ages (light grey ellipses in Fig. 2) are older than rim ages, yielding a weighted average (MSWD 1.7) of 492 ± 12 Ma from 11 analyses (ages younger than 1000 Ma are calculated using the ^{207}Pb-corrected $^{206}Pb/^{238}U$ ratios).

Despite the analytical efforts reduce the errors in the $^{206}Pb/^{238}U$ ratio measurements, the low U content (< 20 p.p.m.) of the central zones resulted in relatively large errors, making in some cases difficult to distinguish between core and rim ages which overlap within analytical error. Nevertheless, nine analyses (two of them rejected) of black rims yield a more precise concordia age (*sensu* Ludwig, 1998) of 483 ± 4 Ma, MSWD 0.025 (white ellipse in Fig. 5). This age is 15–20 Ma younger than the well-established age of the gabbroic intrusion (see previous section), and is therefore interpreted as representing a distinct younger event. We interpret it as a result of metamorphic growth of zircon during the development of the granulitic fabric and concomitant crustal thickening (see Abati *et al.*, 2003 for details on the metamorphic evolution of these rocks). The systematic trend of younger ages in zircon rims can be visualized in the CL pictures of Fig. 2. Additionally, a reconnaissance trace element study (see analytical methods and Table 4 in the Electronic Appendices) shows a marked difference Yb, Er and Hf contents between cores (lower values) and rims (higher values), consistent with a high-temperature metamorphism event for the origin of the rims (Hoskin and Schaltegger, 2003).

Discussion

The precise knowledge of the tectonothermal history of the sampled granulites together with the study of the internal features on zircons revealed by CL has permitted us to constrain two high-temperature events virtually coeval, close to the resolution limit of the method. We used the most concordant analyses of zircons with metamorphic characteristics from sample G97 to obtain the age of the high-temperature metamorphism imprinted by the gabbro intrusion in the pelitic granulite (505 ± 2 Ma). This age is slightly older than the previously reported age for the magmatism (499 ± 2 Ma, ID-TIMS in zircons from the Monte Castelo gabbro, Abati *et al.*, 1999); however, in Fig. 4b, it can be clearly seen that, in spite of the statistical improvement in the error of the SHRIMP mean age

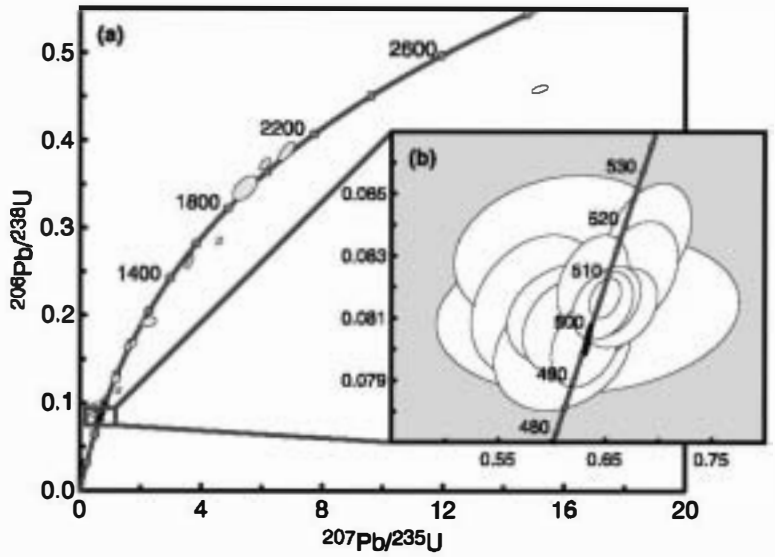

Fig. 4 (a) Concordia plot showing distribution of SHRIMP zircon analyses from a metapelitic granulite included in the Monte Castelo gabbro (sample G97). (b) Cluster of most concordant analyses at 505 ± 2 Ma (white ellipses), interpreted as the age of the high-temperature metamorphism in the metapelite due to the gabbro intrusion. The data obtained from zircons of the Monte Castelo gabbro (black ellipses) is also included for comparison. Error ellipses are $\pm 1\sigma$ for SHRIMP analyses and $\pm 2\sigma$ for ID-TIMS analyses. Isotopic ratios plotted are ^{204}Pb-corrected for common lead.

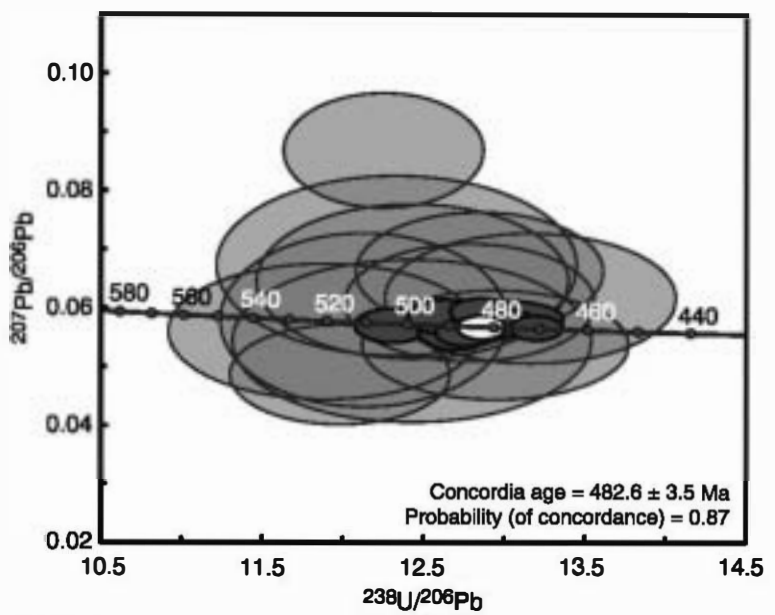

Fig. 5 Tera-Wasserburg plot showing SHRIMP U Pb zircon ages from a granulitic shear zone cross-cutting the Monte Castelo gabbro (sample OW165). Light grey ellipses, cores; dark grey ellipses, black rims; white ellipse, concordia age of the rim analyses. Error ellipses are $\pm 1\sigma$. Isotopic ratios plotted are uncorrected for common Pb.

calculated by ISOPLOT, most of the individual data error ellipses overlap with the previous geochronological data, leading us to consider both ages equivalent and to interpret them as the age of the intrusion of the Monte Castelo gabbro which induced high-temperature metamorphism in the metapelitic xenolith prior to its burial.

In the mafic granulite, the results obtained in the zircon magmatic cores (492 ± 12 Ma) are interpreted as the age of plutonism, in agreement with previous results, even though the low U content resulted in a big error. The age recorded in the black rims (483 ± 4 Ma) is significantly younger than the tightly constrained crystallization age of the gabbro. In spite of the high Th/U values obtained from these black rims, we interpreted them as metamorphic overgrowths because they are absent in the zircons from the non-metamorphosed gabbro, precluding a late magmatic origin (Pidgeon, 1992). Therefore, the use of the low Th/U ratios as a clear discriminant of metamorphic zircon (e.g. Rubatto, 2002) must be re-evaluated, as high Th/U values are usual in metamorphic zircons (e.g. Fernández-Suárez *et al.*, 2007; for a discussion see Harley *et al.*, 2007).

These ages show the intimate relationship between the magmatic heat production and the development of high-temperature regional metamorphism, and the relative synchronicity of igneous activity, burial and deformation in the deep parts of the arc environments. The close spatial and temporal relationship between deformation and emplacement of igneous bodies is considered to be a characteristic of magmatic arcs (e.g. Komatsu *et al.*, 1989; Klepeis *et al.*, 2003).

From the regional point of view, the IP units are interpreted as a fragment of a Cambro-Ordovician magmatic arc developed in the peri-Gondwanan realm and incorporated to the Variscan orogenic wedge, which mostly escaped the subsequent deformation events that affected the underlying units. The lower part of the same arc crust is represented by the HP–HT units. A hypothesis that considered the IP units to be a magmatic arc with coeval magmatism, deformation and metamorphism was proposed by Abati *et al.* (1999), based on U–Pb ID-TIMS data. The results presented here support this idea, as they demonstrate that deformation (granulite-facies shearing) immediately follows the intrusion of igneous bodies, and that these features were not overprinted by subsequent Variscan deformation.

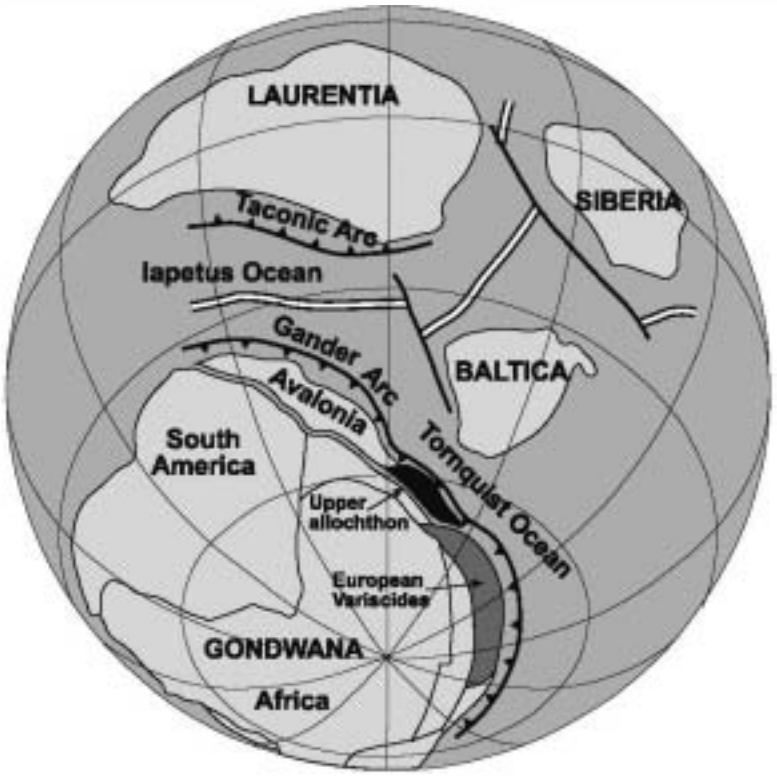

Fig. 6 Schematic reconstruction of distribution of continental masses at Cambro-Ordovician times, showing the suggested palaeopositions of the European Variscides (dark grey) and the exotic terrane where the Monte Castelo gabbro intruded (black). After Gómez Barreiro *et al.* (2007), based on Winchester *et al.* (2002).

Allochthonous terranes overlying the Rheic Ocean suture, as the Upper units of the AC, can be found in several Variscan massifs of Europe, from the French Massif Central to the easternmost realms, like the Góry-Sowie Massif in the Polish Sudetes (Franke and Zelazniewicz, 2000). This continuity suggests that this allochthon could represent a relatively large terrane, even taking into account the dismembering effects of late-Variscan strike-slip tectonics (Shelley and Bossière, 2002; Martínez Catalán *et al.*, 2007). Detrital zircon and inheritance geochronology studies indicate that this terrane originated during the Neoproterozoic–early Palaeozoic in the periphery of the West African Craton (e.g. Fernández-Suárez *et al.*, 2003; Kober *et al.*, 2004). The presence of a Cambro-Ordovician active magmatic arc in this part of the peri-Gondwanan realm is being progressively accepted by an increasing number of authors, linking the *c.* 500 Ma magmatic rocks in correlative terranes with arc environments (e.g. Chen *et al.*, 2000). Consequently, this arc should be taken into account in plate tectonic model reconstructions for the area (Fig. 6). The presence of a magmatic arc system in the north Gondwana margin simultaneous to the rifting process that produced the opening of the Rheic Ocean (e.g. Murphy *et al.*, 2004) provides a mechanism for the initial stages of the process, suggesting that it began as a back-arc rift. Consequently, we propose that the upper allochthon constitutes a remnant of an independent Gondwanan terrane, interpreted as a magmatic arc. A more detailed description of this new terrane and its geological evolution is given by Gómez Barreiro *et al.* (2007). It would be a lateral equivalent of Avalonia and its associated Gander arc that probably drifted away from northern Gondwana around the Cambro-Ordovician boundary, and accreted to the Baltic part of Laurussia during the Silurian (e.g. Murphy *et al.*, 2004). Rift-drift of the terrane represented by the upper allochthon was probably induced by slab roll back of subducting Tornquist oceanic lithosphere (Sánchez Martínez *et al.*, 2007), as the terrane registered voluminous arc plutonism which is at the origin of an early thermal event.

Acknowledgements

This study was financially supported through project CGL2004-04306-C02/BTE of Spanish DGI, and was done while P.C. was holding a Fulbright postdoctoral fellowship at University of Colorado, financed by Spanish Ministerio de Educación y Ciencia. P.C. and J.B.G. are grateful to the people at SUMAC facility for their assistance during the SHRIMP analytical sessions. P.C. thanks I. Brownfield, at the USGS-Denver Microbeam Laboratory, for her help during the CL imaging of the zircons. J. Paces, J. Aleinikoff and W. Premo are thanked for providing the necessary equipment to prepare and image the SHRIMP mounts. Reviews by D. Rubatto, J. Munha and an anonymous reader helped to improve this manuscript and are greatly appreciated.

References

Abati, J., Dunning, G.R., Arenas, R., Díaz García, F., González Cuadra, P. and Martínez Catalán, J.R., 1999. Early Ordovician orogenic event in Galicia (NW Spain): evidence from U–Pb ages in the uppermost unit of the Ordenes Complex. *Earth Planet. Sci. Lett.*, **165**, 213–228.

Abati, J., Arenas, R., Martínez Catalán, J.R. and Díaz García, F., 2003. Anticlockwise *P–T* path of granulites from the Monte Castelo Gabbro (Ordenes Complex, NW Spain). *J. Petrol.*, **44**, 305–327.

Andonaegui, P., González del Tánago, J., Arenas, R., Abati, J., Martínez Catalán, J.R., Peinado, M. and Díaz García, F., 2002. Tectonic setting of the Monte Castelo gabbro (Ordenes Complex, northwestern Iberian Massif): evidence for an arc-related terrane in the hanging wall to the Variscan suture. In: *Variscan–Appalachian Dynamics: The Building of the Late Paleozoic Basement* (J.R. Martínez Catalán, R.D. Hatcher, R. Arenas and F. Díaz García, eds). *Geol. Soc. Am. Spec. Pap.*, **364**, 37–56.

Baba, S., 1998. Proterozoic anticlockwise *P–T* path of the Lewisian Complex of

South Harris, Outer Hebrides, NW Scotland. *J. Metamorph. Geol.*, **16**, 819–841.

Castiñeiras, P., 2005. *Origen y evolución tectonotermal de las unidades de O Pino y Cariño (Complejos Alóctonos de Galicia)*. Ediciós do Castro, A Coruña.

Chen, F., Hegner, E. and Todt, W., 2000. Zircon ages and Nd isotopic and chemical compositions of orthogneisses from the Black Forest, Germany: evidence for a Cambrian magmatic arc. *Int. J. Earth Sci.*, **88**, 791–802.

Corfu, F., Hanchar, J.M., Hoskin, P.W.O. and Kinny, P., 2003. Atlas of zircon textures. In: *Zircon* (J.M. Hanchar and P.W.O. Hoskin, eds). *Rev. Mineral. Geochem.*, **53**, 468–500.

Corona-Chávez, P., Poli, S. and Bigioggero, B., 2006. Syn-deformational migmatites and magmatic-arc metamorphism in the Xolapa Complex, southern Mexico. *J. Metamorph. Geol.*, **24**, 169–191.

Díaz García, F., Martínez Catalán, J.R., Arenas, R. and González Cuadra, P., 1999. Structural and kinematic analysis of the Corredoiras Detachment: evidence for early variscan orogenic extension in the Ordenes Complex, NW Spain. *Int. J. Earth Sci.*, **88**, 337–351.

Fernández-Suárez, J., Corfu, F., Arenas, R., Marcos, A., Martínez Catalán, J.R., Díaz García, F., Abati, J. and Fernández, F.J., 2002. U–Pb evidence for a polyorogenic evolution of the HP–HT units of the NW Iberian Massif. *Contrib. Mineral. Petrol.*, **143**, 236–253.

Fernández-Suárez, J., Díaz García, F., Jeffries, T.E., Arenas, R. and Abati, J., 2003. Constraints on the provenance of the uppermost allochthonous terrane of the NW Iberian Massif: inferences from detrital zircon U–Pb ages. *Terra Nova*, **15**, 138–144.

Fernández-Suárez, J., Arenas, R., Abati, J., Martínez Catalán, J.R., Whitehouse, M.J. and Jeffries, T.E., 2007. U–Pb chronometry of polymetamorphic high-pressure granulites: an example from the allochthonous terranes of the NW Iberian Variscan belt. In: *4-D Framework of Continental Crust* (R.D. Hatcher Jr, M.P. Carlson, J.H. McBride and J.R. Martínez Catalán, eds). *Geol. Soc. Am. Mem.*, **200**, in press.

Flowers, R.M., Bowring, S.A., Tulloch, A.J. and Klepeis, K.A., 2005. Tempo of burial and exhumation within the deep roots of a magmatic arc, Fiordland, New Zealand. *Geology*, **33**, 17–20.

Franke, W. and Zelazniewicz, A., 2000. The eastern termination of the Variscides: terrane correlation and kinematic evolution. In: *Orogenic Processes: Quantification and Modelling in the Variscan Belt* (W. Franke, V. Haak, O. Oncken and D. Tanner, eds). *Geol. Soc. London Spec. Publ.*, **179**, 63–86.

Girardeau, J. and Gil Ibarguchi, I., 1991. Pyroxenite-rich peridotites of the Cabo Ortegal Complex (Northwestern Spain): evidence for large-scale upper-mantle heterogeneity. *J. Petrol.*, **32** (Special Lherzolites Issue), 135–154.

Gómez Barreiro, J., Wijbrans, J.R., Castiñeiras, P., Martínez Catalán, J.R., Arenas, R., Díaz García, F. and Abati, J., 2006. $^{40}Ar/^{39}Ar$ laserprobe dating of mylonitic fabrics in a polyorogenic terrane of NW Iberia. *J. Geol. Soc. London*, **163**, 61–73.

Gómez Barreiro, J., Martínez Catalán, J.R., Arenas, R., Castiñeiras, P., Abati, J., Díaz García, F. and Wijbrans, J.R., 2007. Tectonic evolution of the upper allochthon of the Órdenes Complex (northwestern Iberian Massif): structural constraints to a polyorogenic peri-Gondwanan terrane. In: *The Evolution of the Rheic Ocean: From Avalonian–Cadomian Active Margin to Alleghenian–Variscan Collision* (U. Linnemann, R.D. Nance, P. Kraft and G. Zulauf, eds). *Geol. Soc. Am. Spec. Pap.*, **423**, 315–332.

Harley, S., Kelly, N.M. and Möller, A., 2007. Zircon behaviour and the thermal histories of mountain chains. *Elements*, **3**, 25–30.

Holbrook, W.S., Lizarralde, D., McGeary, S., Bangs, N. and Diebold, J., 1999. Structure and composition of the Aleutian island arc and implications for continental crustal growth. *Geology*, **27**, 31–34.

Hoskin, P.W.O. and Schaltegger, U., 2003. The composition of zircon and igneous and metamorphic petrogenesis. In: *Zircon* (J.M. Hanchar and P.W.O. Hoskin, eds). *Rev. Mineral. Geochem.*, **53**, 27–62.

Klepeis, K.A., Clarke, G.L. and Rushmer, T., 2003. Magma transport and coupling between deformation and magmatism in the continental lithosphere. *GSA Today*, **13**, 4–11.

Kober, B., Kalt, A., Hanel, M. and Pidgeon, R.T., 2004. SHRIMP dating of zircons from high-grade metasediments of the Schwarzwuald/SW-Germany and implications for the evolution of the Moldanubian basement. *Contrib. Mineral. Petrol.*, **147**, 330–345.

Komatsu, M., Osanai, Y., Toyoshima, T. and Miyashita, S., 1989. Evolution of the Hidaka metamorphic belt, northern Japan. *Geol. Soc. London Spec. Publ.*, **43**, 487–493.

Kretz, R., 1983. Symbols for rock-forming minerals. *Am. Mineral.*, **68**, 277–279.

Ludwig, K.R., 1998. On the treatment of concordant uranium-lead ages. *Geochim. Cosmochim. Acta*, **62**, 665–676.

Martínez Catalán, J.R., Arenas, R., Díaz García, F., Rubio Pascual, F.J., Abati, J. and Marquínez, J., 1996. Variscan exhumation of a subducted Paleozoic continental margin: the basal units of the Ordenes Complex, Galicia, NW Spain. *Tectonics*, **15**, 106–121.

Martínez Catalán, J.R., Díaz García, F., Arenas, R., Abati, J., Castiñeiras, P., González Cuadra, P., Gómez Barreiro, J. and Rubio Pascual, F., 2002. Thrust and detachment systems in the Ordenes Complex (northwestern Spain): implications for the Variscan–Appalachian geodynamics. In: *Variscan–Appalachian Dynamics: The Building of the Late Paleozoic Basement* (J.R. Martínez Catalán, R.D. Hatcher, R. Arenas and F. Díaz García, eds). *Geol. Soc. Am. Spec. Pap.*, **364**, 163–182.

Martínez Catalán, J.R., Arenas, R., Díaz García, F., Gómez-Barreiro, J., González Cuadra, P., Abati, J., Castiñeiras, P., Fernández-Suárez, J., Sánchez Martínez, S., Andonaegui, P., Gónzalez Clavijo, E., Díez Montes, A., Rubio Pascual, F.J. and Valle Aguado, B., 2007. Space and time in the tectonic evolution of the northwestern Iberian Massif. Implications for the comprehension of the Variscan belt. In: *4-D Framework of Continental Crust* (R.D. Hatcher Jr, M.P. Carlson, J.H. McBride and J.R. Martínez Catalán, eds). *Geol. Soc. Am. Mem.*, **200**, in press.

McNulty, B.A., 1995. Shear zone development during magmatic arc construction; the Bench Canyon shear zone, central Sierra Nevada, California. *Geol. Soc. Am. Bull.*, **107**, 1094–1107.

Murphy, J.B., Pisarevsky, S.A., Nance, R.D. and Keppie, J.D., 2004. Neoproterozoic – Early Paleozoic evolution of peri-Gondwanan terranes: implications for Laurentia–Gondwana connections. *Int. J. Earth Sci.*, **93**, 659–682.

Pidgeon, R.T., 1992. Recrystallisation of oscillatory zoned zircon: some geochronological and petrological implications. *Contrib. Mineral. Petrol.*, **110**, 463–472.

Pin, C., Ortega Cuesta, L.A. and Gil Ibarguchi, J.I., 1992. Mantle-derived, early Paleozoic A-type metagranitoids from the NW Iberian Massif: Nd isotope and trace-element constraints. *Bull. Soc. Géol. France*, **163**, 483–494.

Rubatto, D., 2002. Zircon trace element geochemistry: partitioning with garnet and the link between U–Pb ages and metamorphism. *Chem. Geol.*, **184**, 123–138.

Sánchez Martínez, S., Arenas, R., Díaz García, F., Martínez Catalán, J.R., Gómez Barreiro, J. and Pearce, J.A., 2007. Careon ophiolite, NW Spain: suprasubduction zone setting for the youngest Rheic Ocean floor. *Geology*, **35**, 53–56.

Santos, J.F., Schärer, U., Gil Ibarguchi, J.I. and Girardeau, J., 2002. Genesis of pyroxenite-rich peritotite at Cabo

Ortegal (NW Spain): geochemical and Pb–Sr–Nd isotope data. *J. Petrol.*, **43**, 17–43.

Shelley, D. and Bossière, G., 2002. Megadisplacements and the Hercynian orogen of Gondwanan France and Iberia. In: *Variscan–Appalachian Dynamics: The Building of the Late Paleozoic Basement* (J.R. Martínez Catalán, R.D. Hatcher, R. Arenas and F. Díaz García, eds). *Geol. Soc. Am. Spec. Pap.*, **364**, 209–222.

van Staal, C.R., 2005. The Northern Appalachians. In: *Encyclopedia of Geology* (R.C. Selley, L.R.M. Cocks and I.R. Plimer, eds), pp. 81–91. Elsevier, Oxford.

van Staal, C.R., Dewey, J.F., MacNiocaill, C. and McKerrow, W.S., 1998. The Cambrian–Silurian tectonic evolution of the northern Appalachians and British Caledonides: history of a complex, west and southwest Pacific-type segment of Iapetus. In: *Lyell: The Past is the Key to the Present* (D.J. Blundell and A.C. Scott, eds). *Geol. Soc. London Spec. Publ.*, **143**, 199–242.

Stampfli, G.M. and Borel, G.D., 2002. A plate tectonic model for the Paleozoic and Mesozoic constrained by dynamic plate boundaries and restored synthetic oceanic isochrons. *Earth Planet. Sci. Lett.*, **196**, 17–33.

Will, T.M. and Schmädicke, E., 2003. Isobaric cooling and anti-clockwise P–T paths in the Variscan Odenwald Crystalline Complex, Germany. *J. Metamorph. Geol.*, **21**, 469–480.

Winchester, J.A., Pharaoh, T.C. and Verniers, J., 2002. Palaeozoic amalgamation of Central Europe: an introduction and synthesis of new results from recent geological and geophysical investigations. In: *Palaeozoic Amalgamation of Central Europe* (J.A. Winchester, T.C. Pharaoh and J. Verniers, eds). *Geol. Soc. London Spec. Publ.*, **201**, 1–18.

Yoshino, T. and Takamoto, O., 2004. Crustal growth by magmatic accretion constrained by metamorphic *P–T* paths and thermal models of the Kohistan Arc, NW Himalayas. *J. Petrol.*, **45**, 2287–2302.

Supplementary material

The Electronic Appendix is available at www.blackwellpublishing.com/products/journals/suppmat/TER/TER768/TER768sm.htm.